Journal of Applied Polymer Science

Thermal and mechanical properties of liquid silicone rubber composites filled with functionalized graphene oxide

Xiong-wei Zhao, Chong-guang Zang, Yu-quan Wen, Qing-jie Jiao
State Key Laboratory of Explosive Science and Technology, Beijing Institute of Technology, Beijing 100081, People's Republic of China
Correspondence to: C. Zang (E-mail: zangchongguang@bit.edu.cn)

ABSTRACT: To improve the thermal and mechanical properties of liquid silicone rubber (LSR) for application, the graphene oxide (GO) was proposed to reinforce the LSR. The GO was functionalized with triethoxyvinylsilane (TEVS) by dehydration reaction to improve the dispersion and compatibility in the matrix. The structure of the functionalized graphene oxide (TEVS-GO) was evaluated by Thermogravimetric analysis (TGA), Fourier transform infrared (FTIR) spectra, X-ray diffraction (XRD), and energy dispersive X-ray spectroscopy (EDX). It was found that the TEVS was successfully grafted on the surface of GO. The TEVS-GO/LSR composites were prepared via in situ polymerization. The structure of the composites was verified by FTIR, XRD, and scanning electron microscopy (SEM). The thermal properties of the composites were characterized by TGA and thermal conductivity. The results showed that the 10% weight loss temperature (T_{10}) increased 16.0°C with only 0.3 wt % addition of TEVS-GO and the thermal conductivity possessed a two-fold increase, compared to the pure LSR. Furthermore, the mechanical properties were studied and results revealed that the TEVS-GO/LSR composites with 0.3 wt % TEVS-GO displayed a 2.3-fold increase in tensile strength, a 2.79-fold enhancement in tear strength, and a 1.97-fold reinforcement in shear strength compared with the neat LSR. © 2015 Wiley Periodicals, Inc. J. Appl. Polym. Sci. **2015**, *132*, 42582.

KEYWORDS: composites; grafting; mechanical properties; rubber; thermal properties

Received 10 February 2015; accepted 4 June 2015
DOI: 10.1002/app.42582

INTRODUCTION

Graphene, a class of 2D nanomaterial with a hexagonal lattice array of sp^2 hybridized carbon atoms, has received much attention due to its remarkable electronic,[1] thermal,[2] and mechanical[3,4] properties since it was firstly exfoliated by Geim and coworkers[5] in 2004. Graphene has been used in a variety of applications ranging from electronic science[6] to polymer nanocomposites[7–10] and proposed as an alternative or supplementation to traditional carbon nanotube (CNT) in reinforcements of polymer composites. Several groups have reported that thermal,[11] piezoresistive,[12] mechanical,[13,14] and electrical[6,14] properties of polymer composites were improved by using graphene or GO additives.

However, to a large extent, the applications of graphene/polymer composites were largely limited by the poor dispersibility and compatibility of pristine graphene in the polymer matrix. Owing to the strong intrinsic van der Waals attraction between the sheets and the high surface area, it is difficult for the graphene nanosheets to disperse in the polymer matrix.[15–17] To settle this problem, a common methodology is acid oxidation that induces plenty of oxygen-containing groups on the surface of graphene sheets.[18] The graphene oxide (GO) possesses large possibility to be modified to improve the dispersion and compatibility in the polymer matrix. Scientists have proposed many different surface treatments and functionalization techniques for enhancing the interface interaction of GO with the polymer matrix.[19–22] Among these attempts, polysiloxane are widely applied to modify the graphene sheets. As examples, Li *et al.*[23] synthesized two different silane coupling agents functionalized GO and prepared two kinds of epoxy nanocomposites. Wan *et al.*[24] investigated the surface functionalization of GO with 3-glycidoxypropyltrimethoxy silane coupling agent and fabricated silane-f-GO/epoxy composites.

Thanks to operability and appropriate curring process, liquid silicone rubber (LSR) lends themselves to a broad range of applications, in particular for the sealing of electronic devices. Nevertheless, in general, the poor thermal conductivity of LSR makes it a problem for the coated or potted devices to dissipate the excess heat, thus leading to damage or a reduced lifetime of devices. Moreover, it is necessary to reinforce the mechanical properties of LSR to protect the coated devices. To ease this

current situation, many trials have been attempted.[25–28] As examples, Mu *et al.*[25] researched the thermal conductivity of silicone rubber filled with ZnO in a wide volume range, and studied the effect of formed conductive particle chains on thermal conductivities. Zhou *et al.*[27] prepared Al_2O_3/silicone rubber composites, and investigated the effects of the amounts of Al_2O_3 on thermal conductivity and mechanical properties of silicone rubber. The thermal conductivities of silicone rubber composites reach a big value by filling ZnO, Al_2O_3 or other fillers, but the amounts of fillers are considerable. Moreover, with the addition of fillers loadings, the mechanical properties of silicone rubber composites become worse and worse, and the viscosities of the composites before curring become bigger and bigger, which does not contribute to the utilization. For this, we studied the surface functionalization of GO with triethoxyvinylsilane (TEVS) coupling agent to improve the performance of LSR. The silane functionalized GO (TEVS-GO) can not only enhance the thermal conductivities of LSR composites, but also strengthen the mechanical properties of composites with little loadings. And there is no influence on the viscosity of the composites. The composites with both GO and TEVS-GO were prepared with different fillers loadings. Thermal and mechanical properties of the composites were measured to evaluate the performance of the composites.

EXPERIMENTAL

Materials

Commercial polydimethylvinylsiloxane (PMVS, $M_w = 75{,}300$) and polymethylhydrosiloxane (PMHS, $M_w = 71{,}200$) were purchased from Shangdong Dayi Chemical Co., China. The vinyl content of PMVS is 0.5 mol % and the hydrogen content of PMHS is 0.3 mol %. A platinum catalyst and an inhibitor were synthesized in our laboratory. Natural graphite flakes were supplied by Qingdao Hensen Graphite Co., China. Triethoxyvinylsilane (TEVS), potassium permanganate ($KMnO_4$), sodium nitrate ($NaNO_3$), sulfuric acid (H_2SO_4), hydrogen peroxide (H_2O_2), ethanol, ammonia solution, and toluene were received from Sinopharm Chemical Reagent Beijing Co.

Preparation of GO

Graphene oxide (GO) was prepared by a modified Hummers and Offeman's method.[29,30] 4 g graphite and 4 g $NaNO_3$ were mixed with 160 mL H_2SO_4 in a 1000 mL beaker and stirred uniformly in an ice bath for 15 min, maintaining the temperature at 0°C. Then 16 g $KMnO_4$ was slowly added into the mixture over the course of 10 min while stirring, and the reaction vessel was kept under the ice bath to prevent the temperature from exceeding 20°C. After that, the reaction vessel was transferred to a 30°C water bath, stirring the mixture for about 30 min. Subsequently, 160 mL deionized water was added slowly with strong mechanical stirring to control the temperature below 100°C. Eventually, 500 mL deionized water and 60 mL 30% H_2O_2 were added into the mixture to terminate the reaction. The warm solution was filtered and washed with deionized water repeatedly until the pH value of supernatant reached 6. GO was obtained after drying in a vacuum oven at 60°C.

Preparation of TEVS-GO

100 mg GO was dispersed in 200 mL ethanol through ultrasonication (in a water bath, 40 kHz) for 6 h in a three-neck flask. Then 5 mL TEVS and 0.5 mL ammonia solution were added into the mixture. After that, the mixture was quickly transferred into a water bath with fierce stirring at 65°C for 48 h under reflux. The reacted GO was filtered and washed with ethanol 3–5 times to remove the unreacted TEVS molecules. Afterwards it was dried in a vacuum oven at 60°C. The functionalized GO was obtained and assigned as TEVS-GO [as shown in Figure 1(a)].

Preparation of TEVS-GO/LSR and GO/LSR Composites

Figure 1(b) depicts the preparation of TEVS-GO/LSR composites. As a typical procedure, TEVS-GO was dispersed in toluene for 2 h through ultrasonication to obtain uniform suspension. Then, the suspension was mixed with PMVS (3 : 1 weight ratio). After PMVS was completely dissolved, the mixture was stirred at 70°C until constant weight and a viscous TEVS-GO/PMVS solution was obtained. Next, PMHS, platinum catalyst, and inhibitor were thoroughly mixed with the TEVS-GO/PMVS mixture (the weight ratio of PMVS : PMHS = 1 : 2). After degassed to remove the air bubbles, the mixture was poured into a polytetrafluoroethylene mold and cured for 24 h at 80°C. The TEVS-GO/LSR composites containing 0.05, 0.1, 0.15, 0.2, 0.25, and 0.3 wt % TEVS-GO were prepared by the above mentioned steps, and GO/LSR composites were also obtained by the same method.

Characterization

Thermogravimetric analysis (TGA) was performed with a Netzsch TG 209 F1Iris thermogravimetric analyzer (Selb, Germany) from ambient temperature to 800°C at a heating rate of 10°C min^{-1} under a nitrogen atmosphere. Fourier transform infrared (FTIR) spectra were conducted using an IFS 66V/S FTIR spectrometer (Bruker, Germany). GO and TEVS-GO were separately pressed into pellets with potassium bromide and then scanned from 500 and 4000 cm^{-1} at a resolution of 4.0 cm^{-1}. The composites were scanned directly. X-ray diffraction (XRD) was used for the X-ray analysis via a Bruker D8 Advance X-ray diffractometer using Cu (Kα) radiation ($\lambda = 0.154$ nm) with the step size 0.014° ranging from 5 to 50° at a speed of 2° min^{-1}. GO and TEVS-GO were separately pressed to form a plane for X-ray analysis, and the composites were prepared by curing a plane for testing. Scanning electron microscopy (SEM) and energy dispersive X-ray spectroscopy (EDX) were obtained on a cold field emission scanning electron microscopy (SEM; S4800, Hitachi High-Technologies Corp.). The fracture surfaces of the composites were coated gold before scanning.

To measure the mechanical properties of LSR composites, samples were tested using an Electronic universal testing machine (WDS-10, Beijing Guance Testing Instrument Co.). The tensile strength and elongation at break were measured according to the GB/T 528–2009 of China with a dumbbell specimen. The tear strength was performed in accordance with GB/T 529–2008 (China) with a right-angled shape specimen. And HG/T 3848-2008 (China) was implemented to measure the shear strength with the specimen dimensions 120 × 15 × 10 mm^3. The specimen was sheared three parts by moving up and down of the

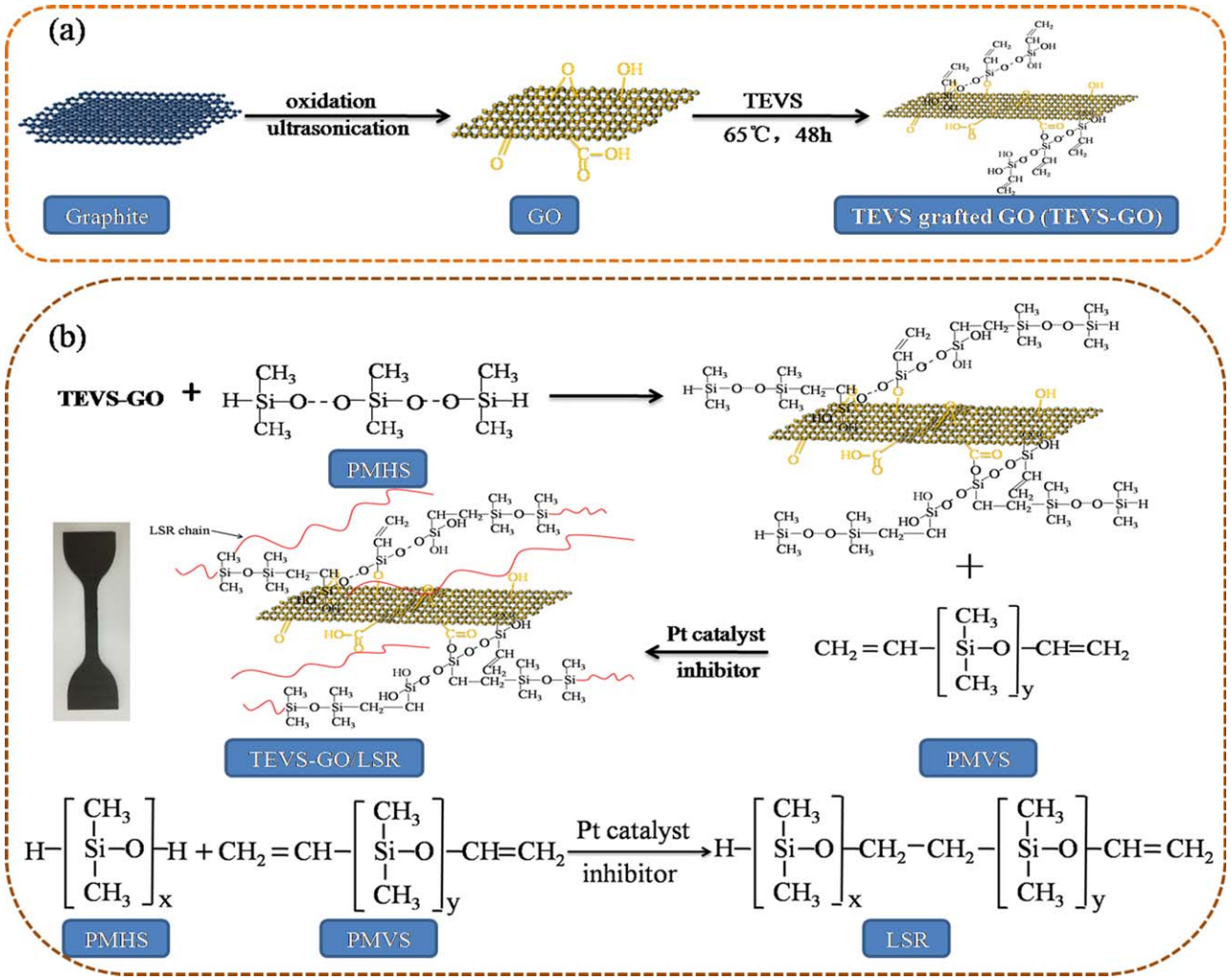

Figure 1. Scheme of procedure for preparation of (a) TEVS-GO and (b) TEVS-GO/LSR composites. [Color figure can be viewed in the online issue, which is available at wileyonlinelibrary.com.]

clamps. Every sample was tested at least five times, and the average value was recorded.

Thermal conductivity of LSR composite was calculated with the following equation in accordance with ASTM E1461:

$$\lambda = \alpha \times \rho \times c_P$$

where λ is the thermal conductivity, α is thermal diffusivity, ρ is density, and c_P is specific heat capacity, respectively. The thermal diffusivity was conducted on a Netzsch LFA 447 system (Selb, Germany) with the temperature ranging from 25 to 150°C. The density was calculated by Archimedean method. The volume was measured by the displacement of water. The weight was tested by an electronic balance. The specific heat capacity was measured by a differential scanning calorimeter (DSC, Netzsch 200 F3 Maia, Selb, Germany) from 25 to 150°C at a heating rate of 10°C min^{-1} under a nitrogen atmosphere.

RESULTS AND DISCUSSION

TGA Analysis

Different materials exhibit distinct thermal stability and thermal decomposition behaviors. Figure 2 presents the TGA curves of graphite, GO, and TEVS-GO. The pristine graphite hardly decomposes till the temperature goes up to 800°C and exhibits high thermal stability.[31] After oxidation, owing to the removal of adsorbed water and decomposition of some oxygen-containing functional groups, GO has a slight weight loss below 150°C. This phenomenon can be observed in our previous work.[32] Afterwards, a significant weight loss appears at temperature between 150 and 260°C, which may be attributable to large decomposition of the unstable oxygen functionalities[24] (such as hydroxyl and carboxylic groups etc.). Compared with the thermal behaviors of graphite and GO, TEVS-GO displays a better thermal stability and undergoes weight loss by three steps. TEVS-GO presents a slighter weight loss below 150°C than GO, demonstrating the change of the sheets surface and decrease of active oxygen-containing functional groups. From 170 to 260°C, the weight loss may result from the degradation of unreacted oxygen-containing functional groups of GO. For the third section, between 260 and 480°C, the weight loss is likely attributed to the decomposition of the grafted TEVS, which demonstrates the existence of TEVS on the surface of GO, modifying the GO surface properties successfully.

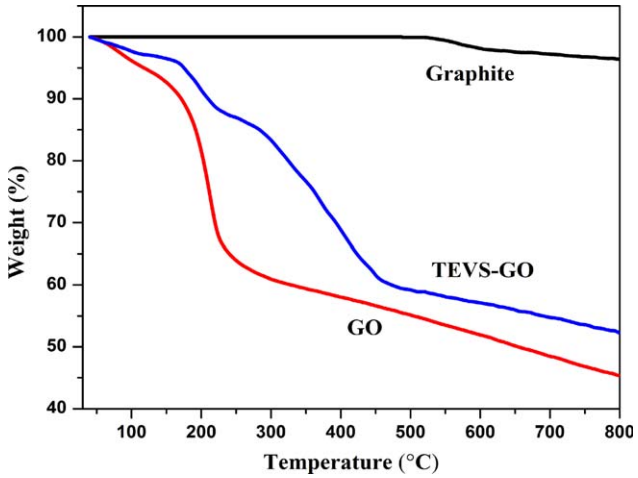

Figure 2. TGA curves of graphite, GO, and TEVS-GO. [Color figure can be viewed in the online issue, which is available at wileyonlinelibrary.com.]

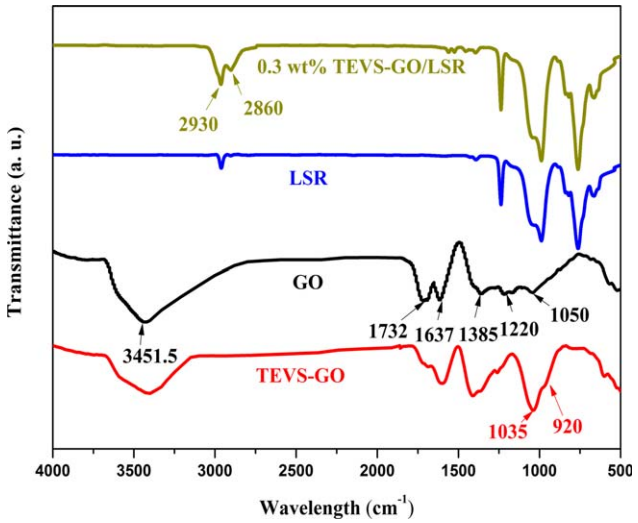

Figure 3. FTIR spectra of GO, TEVS-GO, pure LSR, and 0.3 wt % TEVS-GO/LSR composite. [Color figure can be viewed in the online issue, which is available at wileyonlinelibrary.com.]

FTIR Spectra Analysis

A comparison of FTIR spectra of GO, TEVS-GO, pure LSR, and TEVS-GO/LSR composite are shown in Figure 3. In the case of GO, the stretching vibrations of C=O from carbonyl and carboxylic groups is detected around 1732 cm^{-1}, C=C stretching at 1637 cm^{-1}, O–H stretching at 3451.5 cm^{-1}, C–O vibration of the C–OH at 1220 cm^{-1}, O–H vibration of the C–OH groups at 1385 cm^{-1}, and C–O–C at 1050 cm^{-1}.[33,34] After surface functionalization of TEVS, the band at 3451.5 cm^{-1} becomes weaker, and C–O vibration of the C–OH at 1220 cm^{-1} vanishes, likely resulting from the reaction of C–OH and TEVS. Moreover, two new bands appear at 1035 cm^{-1} and 920 cm^{-1}, corresponding to the stretching of Si–O–Si bond,[34] which is ascribed to the hydroxylation of TEVS molecules in the solution. Therefore, it is reasonable to deduce that the TEVS molecules experience hydrolysis and dehydration. Above all, the disappearance of C–O vibration in C–OH and presence of the stretching of Si–O–Si bond demonstrate the occurrence of a chemical reaction between GO and TEVS. For the TEVS-GO/LSR composite, the absorption band at around 1637 cm^{-1}, which is attributed to $–CH_2=CH_2$ group in TEVS-GO, disappears in the spectra, suggesting the chemical bonding between TEVS-GO and PMHS. Besides, in the FTIR spectra of TEVS-GO/LSR composite, the doublet at 2860 cm^{-1} and 2930 cm^{-1} are observable corresponding to symmetric and asymmetric vibration of $–CH_2–$ groups.[34,35] Compared to the pure LSR, the TEVS-GO/LSR composite exhibits a strong absorption at 2860 cm^{-1} and 2930 cm^{-1}, further demonstrating the occurrence of chemical reaction between TEVS-GO and PMHS and successful preparation of TEVS-GO/LSR composites.

XRD Analysis

Figure 4 displays the X-ray diffractograms pattern of graphite, GO, TEVS-GO, pure LSR, and LSR composites with different fillers. A strong and sharp diffraction of graphite can be observed at 26.3°, corresponding to the diffraction of C (002) plane with a *d*-spacing of 0.339 nm.[32] After oxidation, the peak vanishes, and a new broad peak appearing around $2\theta = 10.8°$ corresponds to the C (002) plane of GO, which indicates that the crystal structure of graphite had been destroyed.[33] Owing to the oxidation, oxygen-containing functional groups insert into the graphite sheets, and the interlayer spacing is expanded to 0.819 nm. After modifying with TEVS, the (002) diffraction peak of GO disappears in the TEVS-GO diffraction pattern, demonstrating the variation of lamellar structure of GO. Moreover, a new broadening peak arises ranging from 6 to 10.5° in the TEVS-GO diffraction pattern, and a sharp peak emerges at approximately 8.9°, corresponding to an interlayer *d*-spacing of 0.993 nm. This result confirms that TEVS is intercalated into the GO sheets further, increasing the interlayer spacing and inducing change of crystal structure of GO, which is consistent with the consequence of TGA and FTIR previously. In case of the pure LSR, due to the scattering of the cured silicon

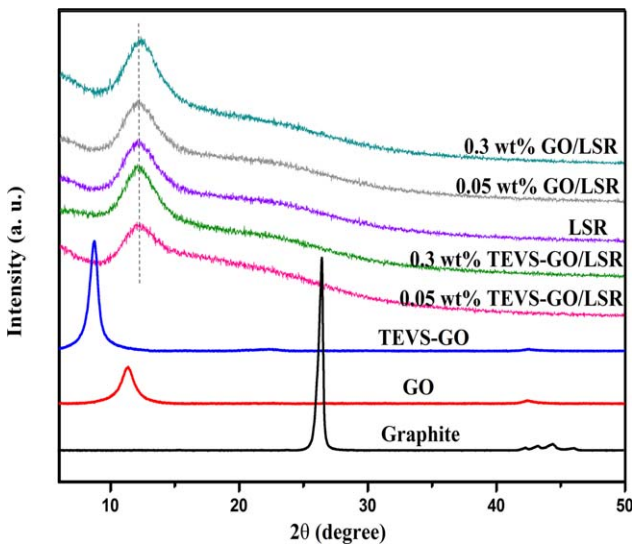

Figure 4. X-ray diffractograms of graphite, GO, TEVS-GO, pure LSR, and LSR composites with different fillers. [Color figure can be viewed in the online issue, which is available at wileyonlinelibrary.com.]

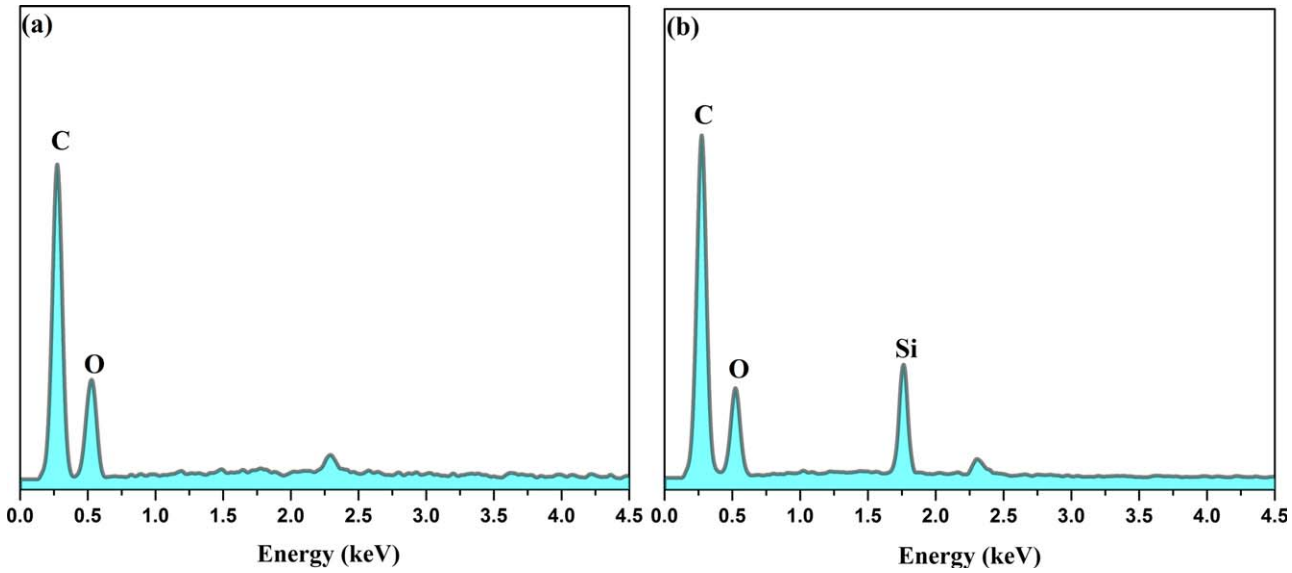

Figure 5. EDX spectra of (a) GO and (b) TEVS-GO. [Color figure can be viewed in the online issue, which is available at wileyonlinelibrary.com.]

molecules, a wide diffraction from 10° to 15° can be observed, revealing its amorphous nature. Note that all the LSR composites filled with GO or TEVS-GO show similar diffraction patterns as the pure LSR. The diffraction peaks corresponding to GO and TEVS-GO are not detected, as indicated by the dotted line in Figure 4, demonstrating the exfoliation of them.[36]

EDX Analysis

Energy dispersive X-ray spectroscopy (EDX) was performed to detect the elemental compositions of materials. Figure 5 presents the EDX spectra of GO and TEVS-GO. The presence of silicon on TEVS-GO is confirmed by the appearance of the Si signal at 1.82 keV,[37] which is consistent with the above discussions. In addition, the atomic percentages of GO and TEVS-GO are summarized in Table I. As can be seen, no silicon signal is detected on GO, yet, 3.09% silicon atomic percentage is tested on TEVS-GO, demonstrating success of modifying. The variations of atomic percentage of C and O reflect the transformation of the functional groups on graphene sheets surface, reacting with TEVS.

Morphology Analysis

To explore the interfacial quality in the polymer composites, the fresh fracture surface of the samples were observed by SEM after a tensile test. The fracture surface of pure LSR is flat and hardly exhibits upheaval [Figure 6(a,b)]. In the GO/LSR composites, a thick sheet structure is observed on the matrix surface at the low magnified SEM image [Figure 6(c)], and the GO aggregations can be seen at the edge of the sheet structure, as directed by the black arrow. At the high magnification image of GO/LSR composites, the same GO aggregates also can be noticed [Figure 6(d)], and some obvious gaps are observed, confirming no interaction between the GO sheets and polymer matrix, as indicated by the arrows. During the failure process, the aggregates and the gaps could induce some micro-cracks to fail the strength of composites. In the case of TEVS-GO/LSR composites, no obvious clusters of TEVS-GO sheets are noticed. The low magnified image of TEVS-GO/LSR composites in Figure 6(e) reveals that a relative good compatibility of TEVS-GO and the polymer matrix is obtained, and no sheet/matrix gaps are observed on the fracture surface, indicating the improvement of interfacial interaction between TEVS-GO and LSR matrix after surface silane functionalization. Furthermore, the contact area of TEVS-GO and LSR matrix is smooth [Figure 6(f)], and some polymer molecules seem to be grafted on the surface of TEVS-GO sheet, as directed by the black arrows. This interaction can promote the local stress transfer between the polymer matrix and sheets efficiently to improve the strength of composites.[23,38]

Thermal Stability of GO/LSR and TEVS-GO/LSR Composites

The thermal stability of GO/LSR and TEVS-GO/LSR composites with different loadings is shown in Figure 7. The 10% weight loss temperature (T_{10}) and the residue at 800°C (R_{800}) are used to evaluate the thermal stability of the composites. As can be seen in Figure 7, the GO/LSR composites show a lower thermal stability than the pure LSR, and the thermal stability decreases with the increase of GO loadings. The T_{10} of the pure LSR starts at 497.5°C, while that of the composites with 0.05 wt % GO at 495.0°C and 0.3 wt % GO at 474.5°C, as listed in Table II. The decrease of initial decomposition temperatures of GO/LSR composites may be related to the degradation of GO.[33] While the TEVS-GO/LSR composites exhibit a higher thermal stability, and the thermal stability increases with the addition of TEV-GO. The T_{10} of TEVS-GO/LSR composites are 500.5°C (0.05 wt % TEVS-GO loading) and 513.5°C (0.3 wt % TEVS-GO loading), respectively. The initial decomposition

Table I. Results of EDX Analysis

Sample	C (atom %)	O (atom %)	Si (atom %)
GO	61.30	38.70	-
TEVS-GO	66.68	30.23	3.09

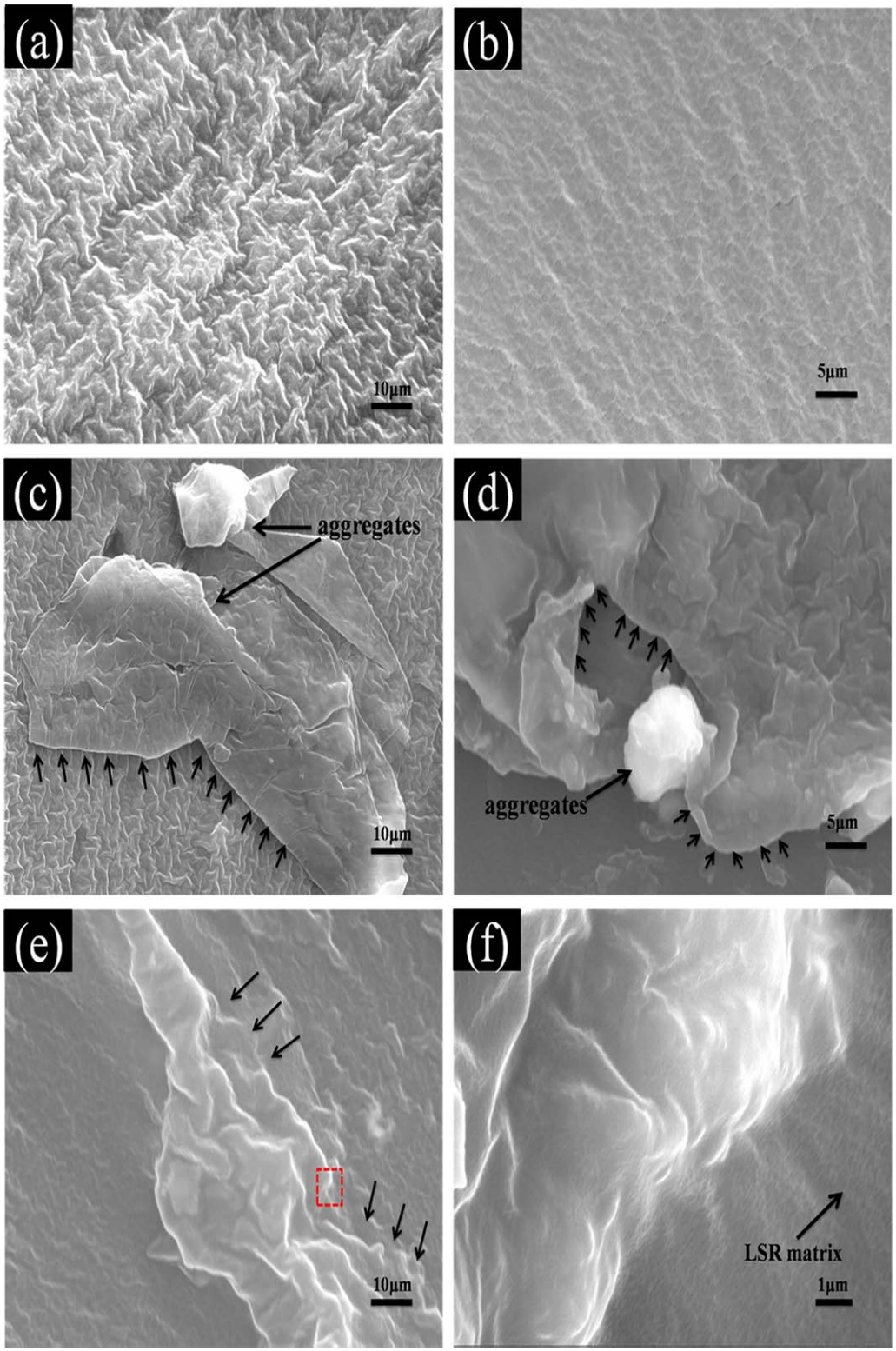

Figure 6. SEM images of fractured surface of (a) ×10.0 k and (b) ×25.0 k of neat LSR, (c) ×10.0 k and (d) ×25.0 k of GO/LSR composites, (e) ×10.0 k and (f) ×60.0 k of TEVS-GO/LSR composites. [Color figure can be viewed in the online issue, which is available at wileyonlinelibrary.com.]

temperature of TEVS-GO/LSR composite increases 16.0°C at 0.3 wt % TEVS-GO loading compared with that of the pure LSR, which may be attributed to the uniformly dispersion of TEVS-GO in the LSR matrix, trammeling the movement of LSR chains to make the thermal decomposition of composites a disadvantage. In addition, the R_{800} of pure LSR is 57.27%, while for the composites 55.98% (0.05 wt % GO/LSR), 50.82% (0.3 wt % GO/LSR), 61.14% (0.05 wt % TEVS-GO/LSR), and

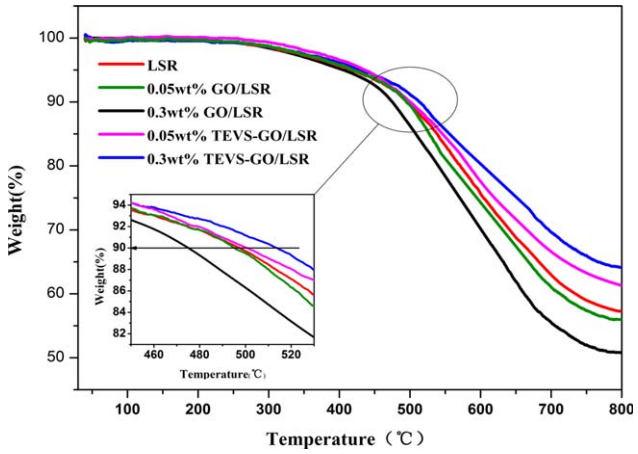

Figure 7. TGA curves of GO/LSR and TEVS-GO/LSR composites with different loadings. Inset is the higher magnification of the referred part as circle indicated. [Color figure can be viewed in the online issue, which is available at wileyonlinelibrary.com.]

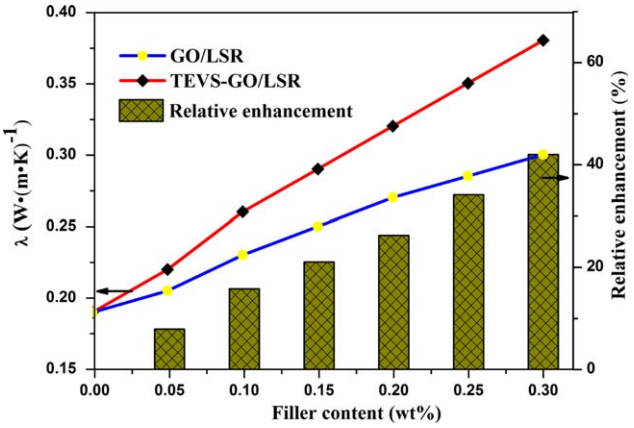

Figure 8. Thermal conductivity of GO/LSR and TEVS-GO/LSR composites with different filler loadings. [Color figure can be viewed in the online issue, which is available at wileyonlinelibrary.com.]

64.17% (0.3 wt % TEVS-GO/LSR), respectively. The tendency of R_{800} is similar to that of T_{10}. The addition of TEVS-GO is beneficial to R_{800} of composites, while the GO decreases R_{800} of composites.

The degradation of pure LSR occurs by two steps: degradation of alkyl groups and degradation of the main chains of siloxane. Due to the energy of silicon–oxygen bond is greater than that of silicon–carbon bond, the silicon–carbon bonds break firstly, when the silicone rubber suffers from heat. The GO contains many oxygen-containing groups, such as –OH, –COOH, and so on. These oxygen-containing groups easily initiate the degradation of alkyl groups, resulting in the degradation of silicone rubber further. Besides, the air in the gaps between GO and the matrix (shown in Figure 6) is another factor to lead to the degradation of the GO/LSR composites. After modified with TEVS, the GO sheets could combine with the chains of siloxane by in situ polymerization, forming chemical crosslinking points and improving the thermal stability of the composites. Moreover, the TEVS-GO could form network in the matrix to act as a barrier to inhibit the emission of volatile degradation products.[35,39]

Thermal Conductivity of GO/LSR and TEVS-GO/LSR Composites

Figure 8 indicates the thermal conductivity of the composites with various loadings of filler at a temperature of 25°C. As we can see, the thermal conductivities of the polymer composites increase with the addition of fillers. At the loading of 0.3 wt %, the thermal conductivity of GO/LSR composites reaches 0.3 W m^{-1} K^{-1}, a moderate potentiation compared to the initial thermal conductivity of LSR (0.19 W m^{-1} K^{-1}). However, at the same loading, the TEVS-GO/LSR composite possesses a thermal conductivity value of 0.38 W m^{-1} K^{-1} (approximate 200% of the neat LSR). Furthermore, with the increase of filler loadings, the thermal conductivities of TEVS-GO/LSR composites are always higher than those of GO/LSR composites, which may associate with the interfacial compatibility and homogeneous dispersion of fillers.[40] The TEVS-GO could boost the thermal conductivity of LSR composites to a same value with lesser filler content than GO, exhibiting high efficiency of enhancement. The relative enhancements TEVS-GO/LSR than GO/LSR composites become from 7.9% (0.05 wt % filler loadings) to 42.1% (0.3 wt % filler loadings). This phenomenon is likely attributable to the formation of thermal conductive network composed by TEVS-GO.

Table II. TGA Data of GO/LSR and TEVS-GO/LSR Composites with Different Loadings

Sample	T_{10} (°C)	R_{800} (%)
Pure LSR	497.5	57.27
0.05 wt % GO/LSR	495.0	55.98
0.3 wt % GO/LSR	474.5	50.82
0.05 wt % TEVS-GO/LSR	500.5	61.14
0.3 wt % TEVS-GO/LSR	513.5	64.17

The conduction of heat is through the atomic vibration along the polymer molecules chains in the LSR matrix, while by electron transfer in GO. Due to the high electron mobility, the graphene has a high thermal conductivity. So, with the addition of fillers, the composites exhibit a higher and higher thermal conductivity. Nevertheless, the aggregates of GO make it a low reinforcement efficiency and the gaps between the GO sheets and polymer matrix prevent the transfer of heat from the polymer molecules chains to the GO sheets in the GO/LSR composites. With the use of TEVS, the vinyl on TEVS-GO could react with the LSR chains directly, linking the GO sheets with the LSR matrix by chemical bonds, which makes it possible to conduct the heat from the polymer molecules chains to the sheets directly, performing a high thermal conductive efficiency. Besides, after modification, the compatibility and dispersibility of GO sheets in the polymer matrix are improved, making for the formation of heat conduction network in the composites to facilitate the heat transmission in the matrix.

Mechanical Properties of GO/LSR and TEVS-GO/LSR Composites

The reinforcing effects of GO and TEVS-GO on the mechanical properties of LSR composites are summarized in Figure 9. With

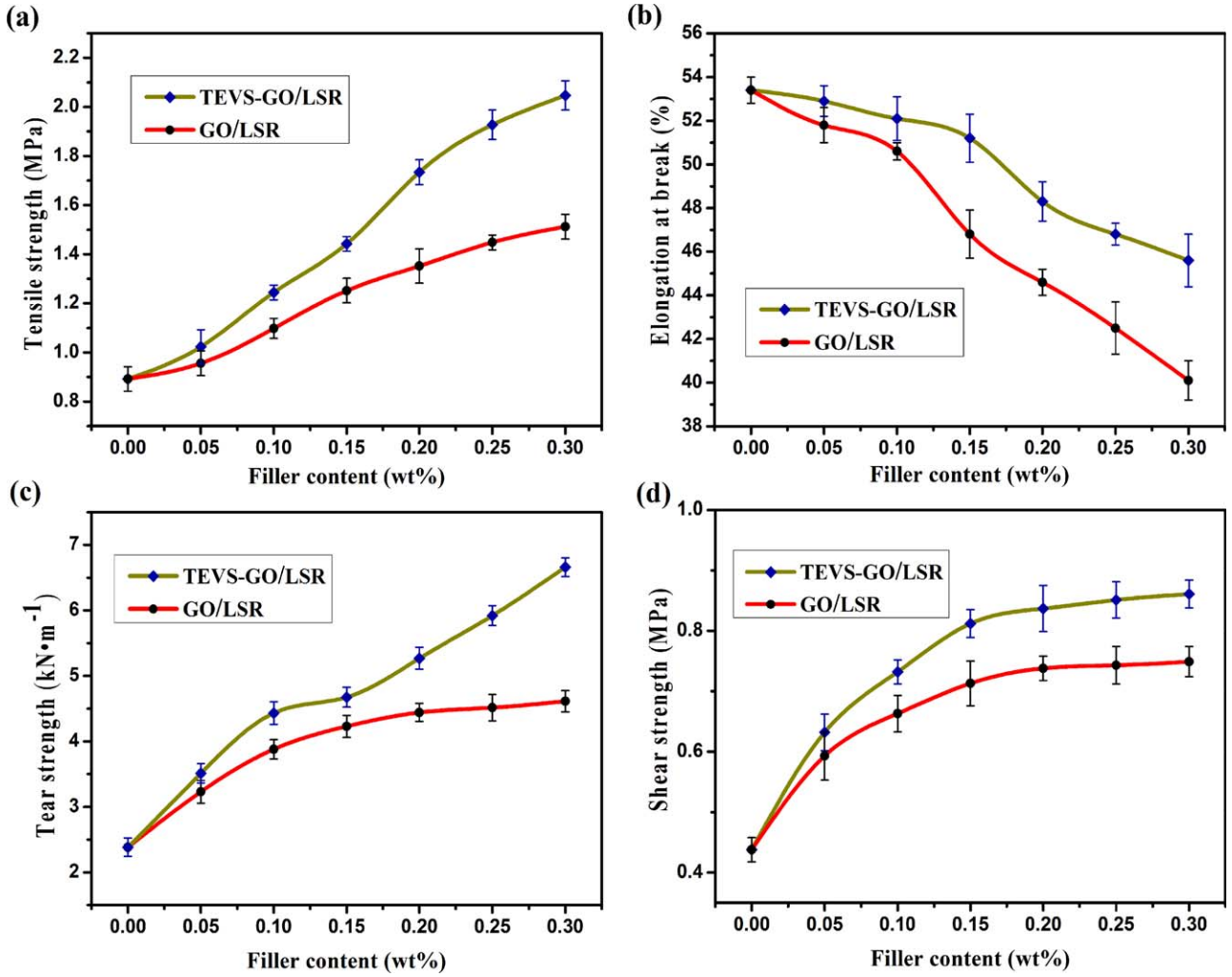

Figure 9. Mechanical properties of GO/LSR and TEVS-GO/LSR composites: (a) tensile strength, (b) elongation at break, (c) tear strength, and (d) shear strength. [Color figure can be viewed in the online issue, which is available at wileyonlinelibrary.com.]

the GO content increasing, the mechanical properties of polymer composites are enhanced, as presented in Figure 9(a,c, and d). The tensile strength, tear strength and shear strength of GO/LSR composites increase from 0.892, 2.383, and 0.438 MPa to 1.512, 4.613, and 0.749 MPa, respectively (approximately 69.51%, 93.58%, and 71.01% increases over the neat LSR, respectively) when the GO content increases from 0 to 0.3 wt %. However, the enhancement of tear strength and shear strength of GO/LSR composites decreases and trends to disappearance after the filler content reaches to 0.15 wt %, which

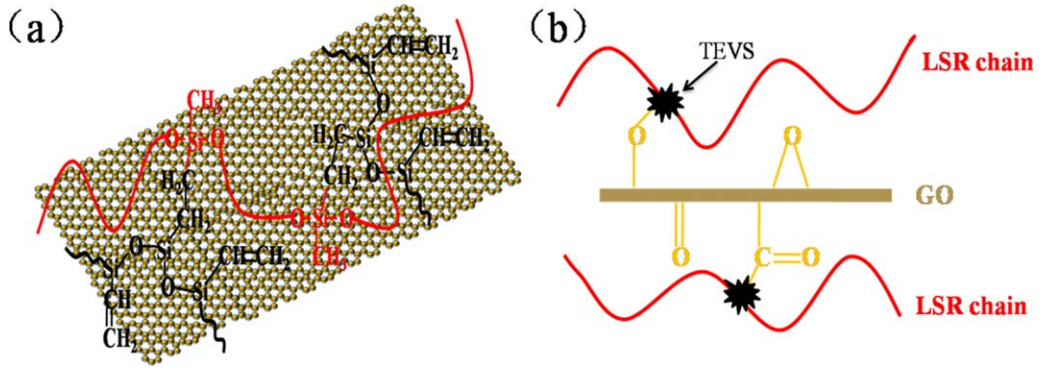

Figure 10. Model structure of TEVS-GO/LSR composites: (a) vertical view and (b) lateral view. [Color figure can be viewed in the online issue, which is available at wileyonlinelibrary.com.]

may result from the filled GO reaching critical content and beginning agglomeration (as observed in the SEM images of Figure 6(c,d)). As the TEVS-GO loading increases from 0 to 0.3 wt %, the tensile strength, tear strength, and shear strength of TEVS-GO/LSR composites increase from 0.892, 2.383, and 0.438 MPa to 2.047, 6.66, and 0.861 MPa, respectively. The improving efficiency of TEVS-GO on mechanical properties is more obvious than that of GO with the same filler loading. Compared with the neat LSR, TEVS-GO/LSR composites with only 0.3 wt % TEVS-GO exhibit a marvelous enhancement in tensile strength (approximately 2.3-fold increase over the neat LSR), tear strength (approximately 2.79-fold increase over the neat LSR), and shear strength (approximately 1.97-fold increase over the neat LSR), revealing that TEVS-GO possesses a high improving efficiency to promote the load transfer. This high-efficiency improvement may be associated with the well-dispersement of TEVS-GO in the polymeric matrix and strong interfaces between TEVS-GO and the LSR matrix (as indicated in the SEM images of Figure 6(e,f)). The elongation at break of both GO/LSR and TEVS-GO/LSR composites decreases with the fillers loading increasing [Figure 9(b)], which may be attributed to low flexibility of GO and TEVS-GO, as well as the poor interfaces of GO and the LSR matrix in GO/LSR composites.

Owing to the interaction of covalent bonds, the TEVS-GO has a high-efficiency improvement on mechanical properties of LSR matrix (Figure 9). Figure 10 shows the interaction of TEVS-GO and LSR chain: (a) vertical view and (b) lateral view. The $-CH=CH_2$ bond on the surface of TEVS-GO can react with the –Si–H bond of PMHS by in situ polymerization under the catalyst, as shown in Figure 10(a). This linkage of the GO sheets and the LSR chains can not only improve the interfacial interaction between the sheets and polymer matrix, but also promote the load transfer. Besides, the existence of TEVS on the graphene sheets surface improves the compatibility of GO sheets and the LSR matrix, decreasing the agglomeration of the sheets in the matrix.

CONCLUSIONS

In summary, a stratagem was proposed via addition of GO functionalized by TEVS to enhance the mechanical properties and thermal properties of LSR composites. Results from TGA, FTIR, XRD, and EDX analysis indicated that the GO sheets were successfully modified by the reaction with TEVS. The SEM images displayed that TEVS-GO exhibited excellent compatibility with the LSR matrix, and strong interfacial interactions between TEVS-GO and the LSR polymeric chain were formed. The thermal stability of LSR was improved by filling TEVS-GO. The thermal conductivity increased from 0.19 W m^{-1} K^{-1} for neat LSR to 0.38 W m^{-1} K^{-1} for the 0.3 wt % TEVS-GO/LSR composite. Furthermore, the 0.3 wt % TEVS-GO/LSR composites, prepared by in situ polymerization, possessed approximately a 2.3-fold increase in tensile strength, a 2.79-fold increase in tear strength, and a 1.97-fold increase in shear strength. The thermal properties and mechanical properties of TEVS-GO/LSR composites exhibited more substantial reinforcement compared to those of GO/LSR composites. Therefore, TEVS-GO was designed as an effective nanofiller to improve the performance of polymeric matrix, and TEVS-GO/LSR with excellent properties was fabricated for a wide range of application.

ACKNOWLEDGMENTS

This work is supported by the Doctoral Fund of Ministry of Education of China (number: 20121101110014).

REFERENCES

1. Chen, W.; Qin, S. Q.; Zhang, X. A.; Fang, J. Y.; Wang, G.; Zhang, S.; Wang, C. C.; Wang, L.; Chang, S. L. *J. Nanosci. Nanotechnol.* **2015**, *15*, 4591.
2. Alexander, A. B.; Suchismita, G.; Bao, W. Z.; Irene, C. *Nano Lett.* **2008**, *8*, 902.
3. Lee, C. G.; Wei, X. D.; Jeffrey, W. K.; James, H. *Science* **2008**, *321*, 385.
4. Frank, I. W.; Tanenbauma, D. M.; Zande, A. M.; McEuen, P. L. *J. Vac. Sci. Technol. B* **2007**, *25*, 2558.
5. Novoselov, K. S.; Geim, A. K.; Morozov, S. V.; Jiang, D.; Zhang, Y.; Dubonos, S. V.; Grigorieva, I. V.; Firsov, A. A. *Science* **2004**, *306*, 666.
6. Castro, N. A. H.; Guinea, F.; Peres, N. M. R. *Rev. Mod. Phys.* **2009**, *81*, 109.
7. Lim, Y. S.; Tan, Y. P.; Lim, H. N.; Tan, W. T.; Mahnaz, M. A.; Talib, Z. A.; Huang, N. M.; Kassim, A.; Yarmo, M. A. *J. Appl. Polym. Sci.* **2013**, *128*, 224.
8. Jang, J. W.; Min, B. G.; Yeum, J. H. *Fiber Polym.* **2013**, *14*, 1332.
9. Deosarkar, M. P.; Pawar, S. M.; Bhanvase, B. A. *Chem. Eng. Process.* **2014**, *83*, 49.
10. Jiang, L.; Shen, X. P.; Wu, J. L.; Shen, K. C. *J. Appl. Polym. Sci.* **2010**, *118*, 275.
11. Li, Q.; Guo, Y. F.; Li, W. W.; Qiu, S. Q.; Zhu, C.; Wei, X. F.; Chen, M. L.; Liu, C. J.; Liao, S. T.; Gong, Y.; Mishra, A. K.; Liu, L. W. *Chem. Mater.* **2014**, *26*, 4459.
12. Cai, W. T.; Huang, Y.; Wang, D. Y.; Liu, C. X.; Zhang, Y. Z. *J. Appl. Polym. Sci.* **2014**, *131*, DOI: 10.1002/app.39778.
13. Shokrieh, M. M.; Esmkhani, M.; Haghighatkhah, A. R.; Zhao, Z. *Mater. Des.* **2014**, *62*, 401.
14. Carolina, F. M.; Fernando, G.; Aldo, J. G. Z. *Carbon* **2014**, *78*, 469.
15. Si, Y.; Samulski, E. T. *Nano Lett.* **2008**, *8*, 1679.
16. Si, Y.; Samulski, E. T. *Chem. Mater.* **2008**, *20*, 6792.
17. Li, D.; Muller, M. B.; Gilje, S.; Kaner, R. B.; Wallace, G. G. *Nat. Nanotechnol.* **2008**, *3*, 101.
18. Jonathan, P. R.; Priyanka, A. P.; Joseph, J. M.; Matthew, B.; Ian, A. K.; Robert, J. Y.; Neil, R. W. *Angew. Chem. Int. Ed.* **2011**, *50*, 3173.
19. Fang, M.; Zhang, Z.; Li, J. F.; Zhang, H. D.; Lu, H. B.; Yang, Y. L. *J. Mater. Chem.* **2010**, *20*, 9635.
20. Manuela, C.; Umar, K.; Toby, S.; Ariene, O. N.; Wang, Z. M.; Ignatius, T. M.; Wolfgang, K. M.; Ana, M. B.; Jonathan, N. C. *Carbon* **2013**, *52*, 363.

21. Lin, Y.; Ehlert, G. J.; Bukowsky, C.; Sodano, H. A. *ACS Appl. Mater. Interfaces* **2011**, *3*, 2200.
22. Yang, H. F.; Li, F. H.; Shan, C. S.; Han, D. X.; Zhang, Q. X.; Niu, L.; Ivaska, A. *J. Mater. Chem.* **2009**, *19*, 4632.
23. Li, Z.; Wang, R. G.; Robert, J. Y.; Deng, L. B.; Yang, F.; Hao, L. F.; Jiao, W. C.; Liu, W. B. *Polymer* **2013**, *54*, 6437.
24. Wan, Y. J.; Gong, L. X.; Tang, L. C.; Wu, L. B.; Jiang, J. X. *Compos. A* **2014**, *64*, 79.
25. Mu, Q. H.; Feng, S. Y.; Diao, G. Z. *Polym. Compos.* **2007**, *28*, 125.
26. Pihale, S.; Eder, F.; Kroke, E. *J. Appl. Polym. Sci.* **2014**, *131*, DOI: 10.1002/app.41037.
27. Zhou, W. Y.; Qi, S. H.; Tu, C. C.; Zhao, H. Z. *J. Appl. Polym. Sci.* **2007**, *104*, 2478.
28. Zhou, W. Y.; Qi, S. H.; Tu, C. C.; Zhao, H. Z.; Wang, C. F.; Kou, J. L. *J. Appl. Polym. Sci.* **2007**, *104*, 1312.
29. Stankovich, S.; Piner, R. D.; Nguyen, S. T.; Ruoff, R. S. *Carbon* **2006**, *44*, 3342.
30. Stankovich, S.; Piner, R. D.; Chen, X. Q.; Wu, N. Q.; Nguyen, S. T.; Ruoff, R. S. *J. Mater. Chem.* **2006**, *16*, 155.
31. Wan, Y. J.; Tang, L. C.; Yan, D.; Zhao, L.; Li, Y. B.; Wu, L. B.; Jiang, J. X.; Lai, G. Q. *Compos. Sci. Technol.* **2013**, *82*, 60.
32. Zang, C. G.; Zhu, X. D.; Jiao, Q. J. *J. Appl. Polym. Sci.* **2015**, *132*, 6230.
33. Wang, X. L.; Dou, W. Q. *Thermochim. Acta.* **2012**, *529*, 25.
34. Ou, J. F.; Wang, J. Q.; Liu, S. L.; Mu, B.; Ren, J. F.; Wang, H. G.; Yang, S. R. *Langmuir* **2010**, *26*, 15830.
35. Wang, X.; Xing, W. Y.; Zhang, P.; Song, L.; Yang, H. Y.; Hu, Y. *Compos. Sci. Technol.* **2012**, *72*, 737.
36. Huang, T.; Lu, R.; Su, C.; Wang, H.; Guo, Z.; Liu, P.; Huang, Z.; Chen, H.; Li, T. *ACS Appl. Mater. Interf.* **2012**, *4*, 2699.
37. Hou, S. F.; Su, S. J.; Kasner, M. L.; Shah, P.; Patel, K.; Madarang, C. *J. Chem. Phys. Lett.* **2010**, *501*, 68.
38. Jiang, T. W.; Kuila, T.; Kim, N. H.; Ku, B. C.; Lee, J. H. *Compos. Sci. Technol.* **2013**, *79*, 115.
39. Pham, V. H.; Dang, T. T.; Hur, S. H.; Kim, E. J.; Chung, J. S. *ACS Appl. Mater. Interfaces* **2012**, *4*, 2630.
40. Yang, S. Y.; Ma, C. C. M.; Teng, C. C.; Huang, Y. W.; Liao, S. H.; Huang, Y. L.; Tien, H. W.; Lee, T. M.; Chiou, K. C. *Carbon* **2010**, *48*, 592.